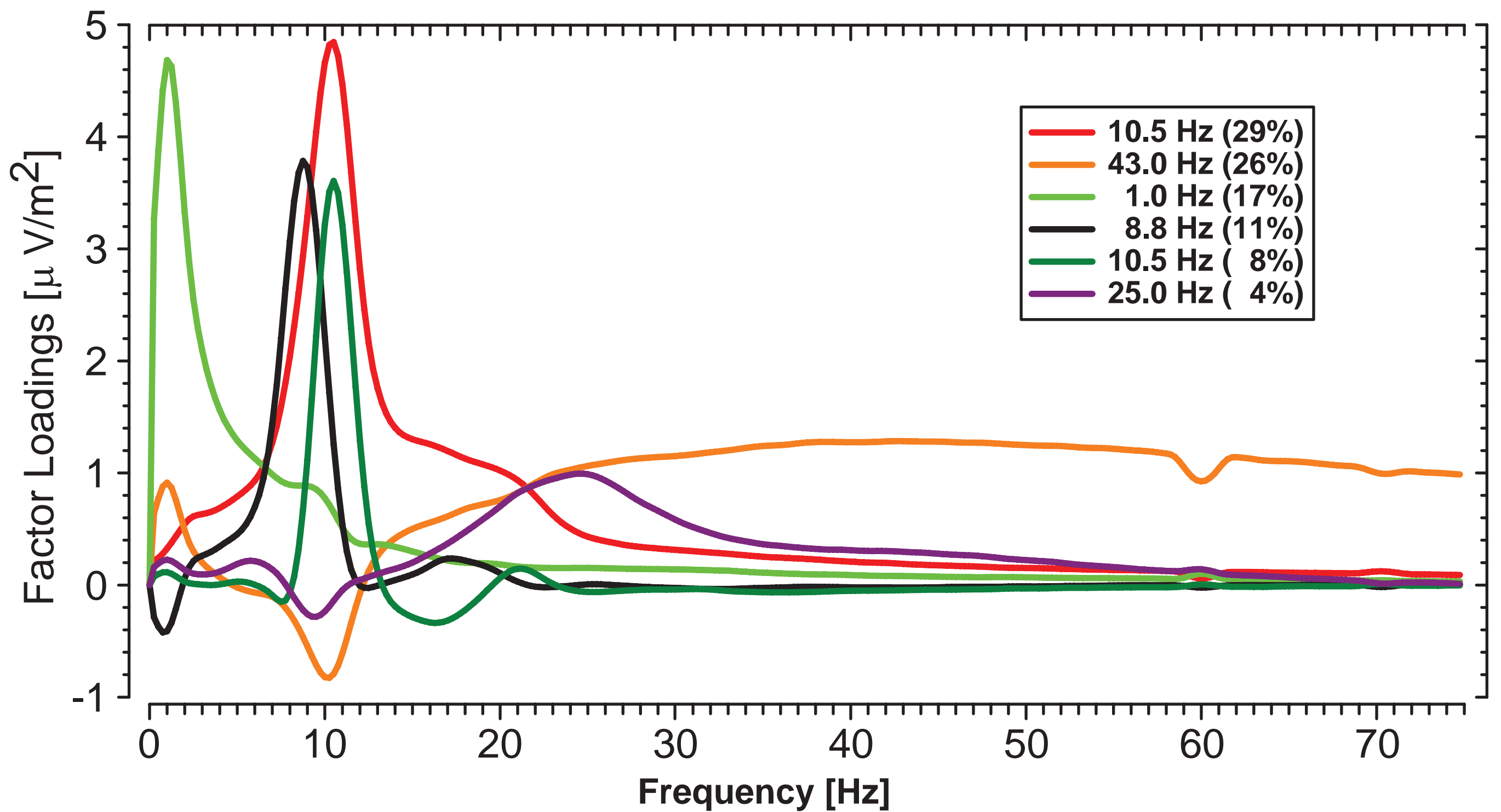
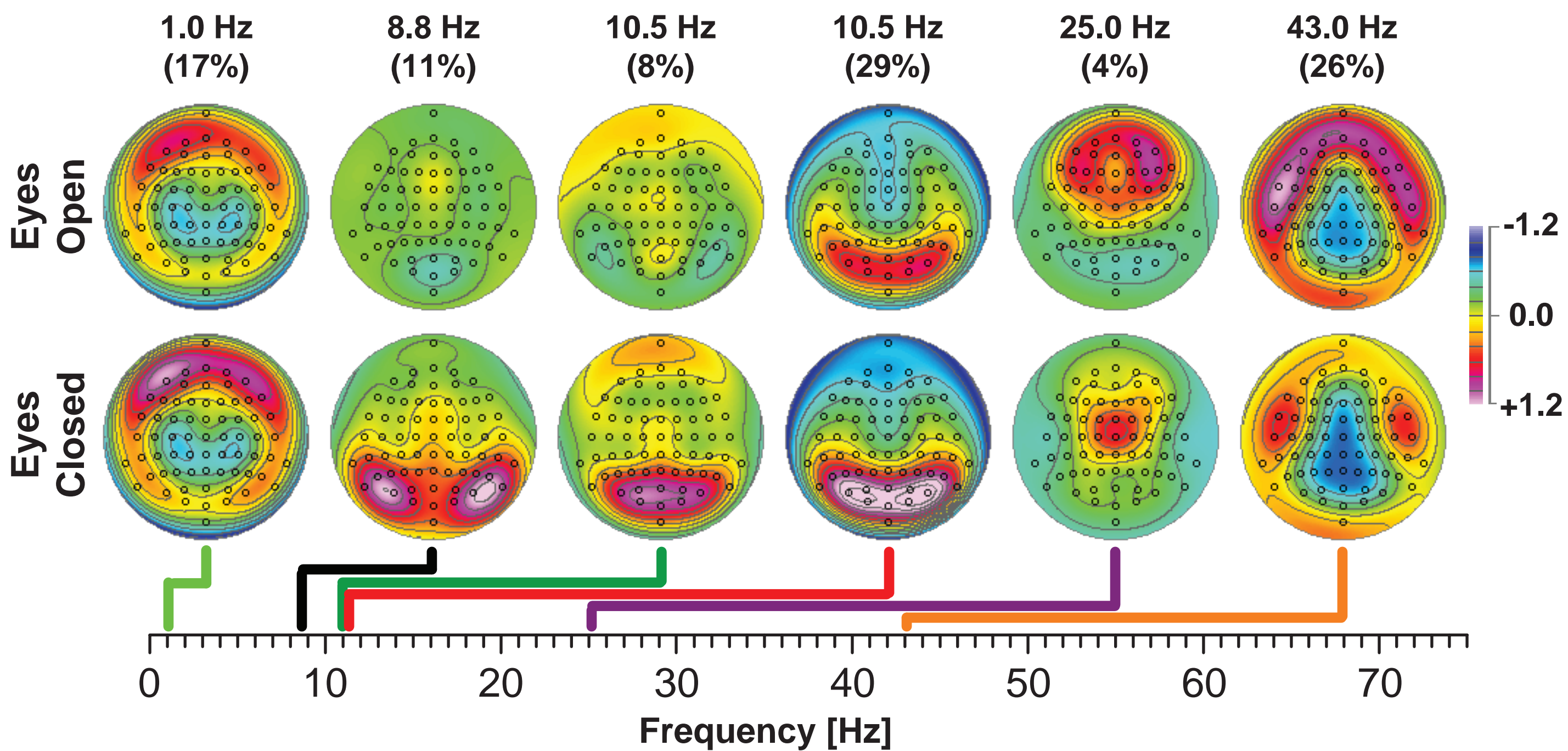


Supplemental Information

Section S1: Overall CSD-fPCA Solution

Averaged CSD amplitude spectra (299 frequency points = variables) were submitted to unrestricted, covariance-based fPCA, with 67 electrodes, 2 conditions, and 82 participants (i.e., 10988 cases), followed by Varimax rotation of the covariance loadings. As shown in Figure S1, six factors accounted for 95% of the variance of amplitude spectra, three of which (48% total variance) had clear peaks in alpha (low-alpha/theta, high-alpha and residual alpha; cf. (1)), and had posterior maxima for eyes-closed.

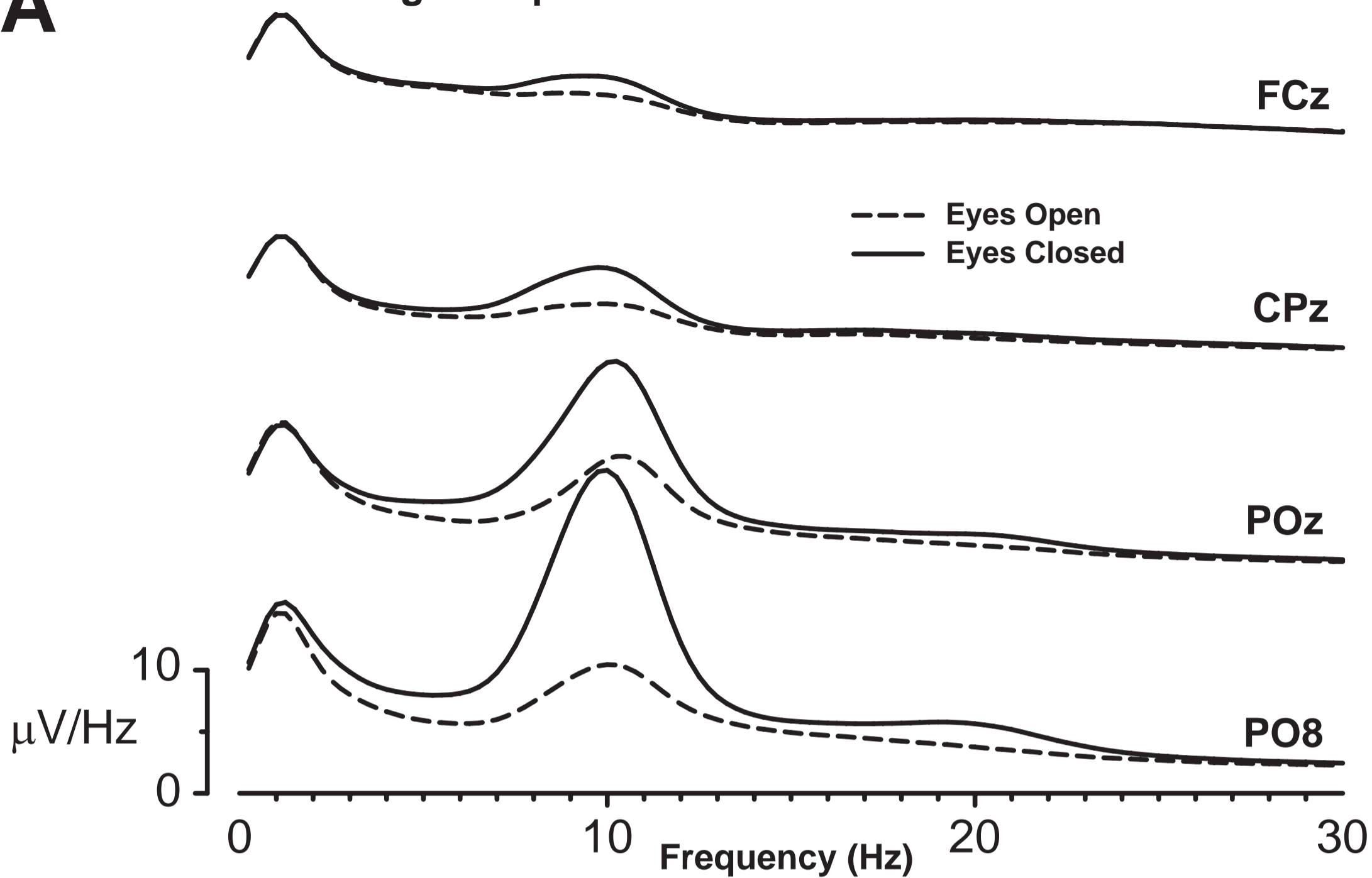
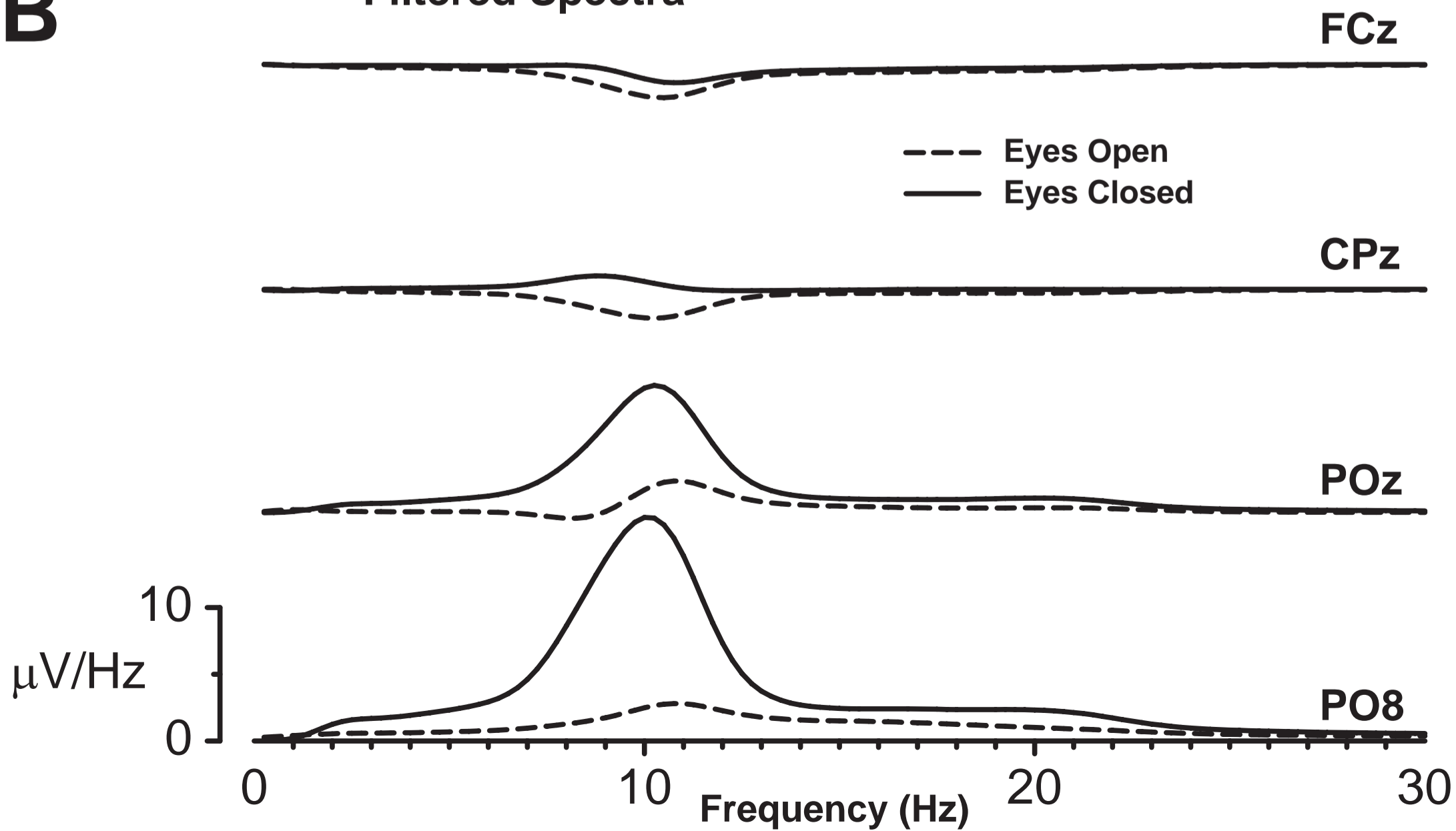
Figure S1. (A) Rotated factor loadings waveforms for the first six CSD-fPCA components derived from the original (unfiltered) data. (B) Corresponding mean factor score topographies for eyes-open and eyes-closed conditions, arranged by loadings peak frequency (coded by line color; e.g., black line: 8.8 Hz peak, 11% amplitude spectrum variance, lateral-posterior eyes-closed topography). Alpha activity was summarized by three factors with 8.8-10.5 Hz peaks. Dots indicate the spherical positions of electrodes (nose at top). Colored lines below maps point to the peak frequencies of corresponding factor loadings waveforms on the common abscissa.

A**B**

Section S2: Reconstruction of Amplitude Spectra from CSD-fPCA Alpha Factors

Preliminary comparisons of the CSD-fPCA factor loadings waveforms for the three alpha factors in Figure S1 (8-12 Hz peaks) with those extracted separately for controls and patients indicated variability in the residual alpha factor loadings for patients (i.e., correlation between overall and patient residual alpha waveforms was $< .7$, compared to $> .95$ for all others). This inconsistency was eliminated by using these three factors as a spectral filter (correlation of alpha factor loadings all $> .994$), resulting in reconstructed amplitude spectra (summation of the products of factor scores and loadings waveforms across the three alpha factors) for each subject and condition. This approach serves as an effective alpha-pass filter that exploits the capacity of fPCA to remove overlapping broadband components (e.g., eye and muscle artifact) from the analysis. The final fPCA factors are reminiscent of those observed for factors produced by band-limiting the original, unfiltered spectra to 5-15 Hz (i.e., others set to zero).

Figure S2. (A) Grand averaged CSD spectra showing greater alpha amplitude for eyes-closed (solid lines) than eyes-open (dashed lines) conditions at midline (FCz, CPz, POz) and right posterolateral (PO8) sites. (B) Corresponding filtered amplitude spectra show preserved alpha, but activity and artifact at lower and higher frequencies is eliminated.

A**Original Spectra****B****Filtered Spectra**

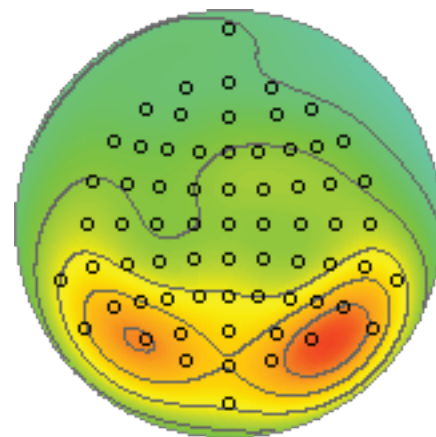
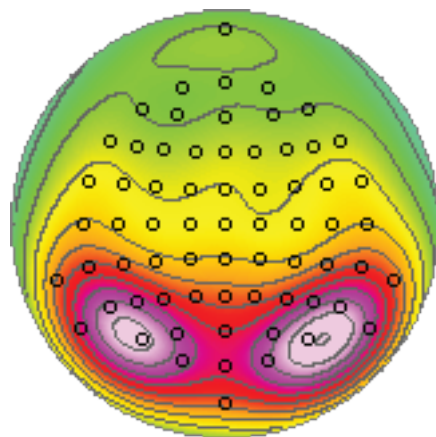
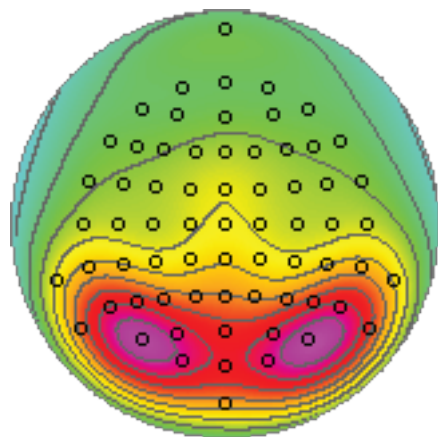
Section S3: Separate Contributions of Low-Alpha/Theta and High Alpha

Low-alpha/theta and high-alpha were both maximal for the eyes-closed condition in posterior regions, but the topographic maximum of high-alpha was at the midline, and the maximum of low-alpha/theta was posterolateral, with a shallow anterior midline secondary topography (Figure S3). Although *Group* trends were evident for the averaged factor score topographies of both factors, the main ANOVA model showed no significant *Group* interaction with *Alpha Frequency* (maximum effect is *Condition x Alpha Frequency x Group*: $F_{[2,75]} = .613$; $p > .5$). However, an exploratory analysis indicated a statistical trend for condition-dependent low-alpha/theta (*Group x Condition*: $F_{[2,75]} = 2.47$; $p = .083$), but not for high-alpha (*Group x Condition*: $F_{[2,75]} = 1.93$, $p > .3$). A separate model for anterior midline low-alpha/theta (Fz, FCz) showed no *Group* effects (maximal *Group* effect or interaction was *Group*: $F_{[1,75]} = .93$, $p = .4$)

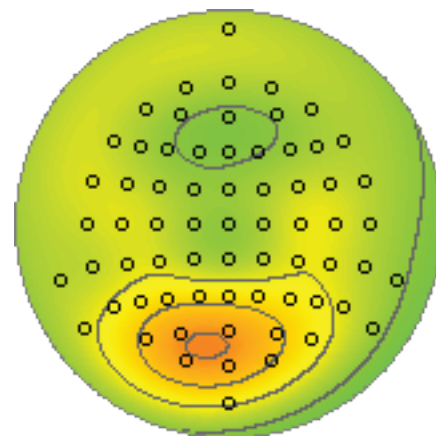
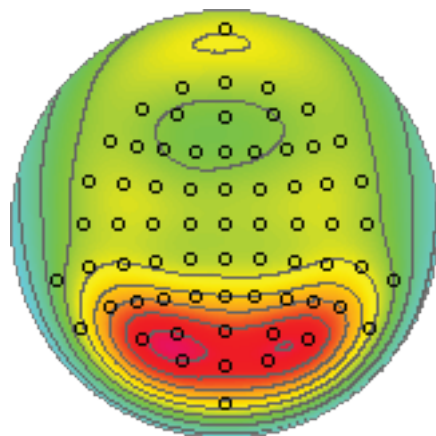
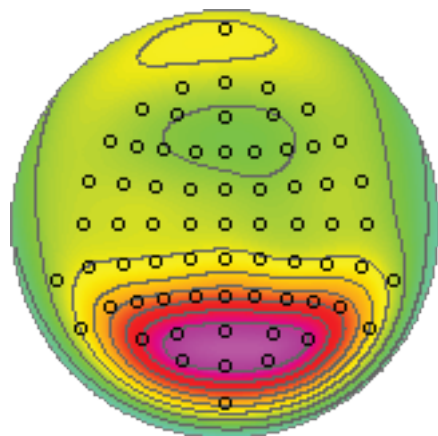
Figure S3. Averaged eyes-closed factor score topographies of low alpha/theta and high-alpha factors for control, responder and nonresponder groups. Both alpha factors showed marked attenuation for nonresponders, despite comparable topographies across groups.

Factor Score Topographies (Eyes Closed)

**Low Alpha/Theta
(9.0 Hz; 50%)**



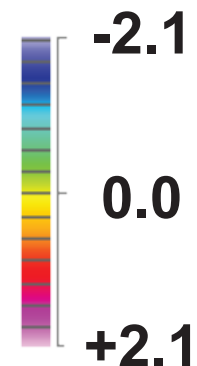
**High Alpha
(10.5 Hz; 34%)**



**Controls
(*n* = 41)**

**Responders
(*n* = 28)**

**Nonresponders
(*n* = 13)**

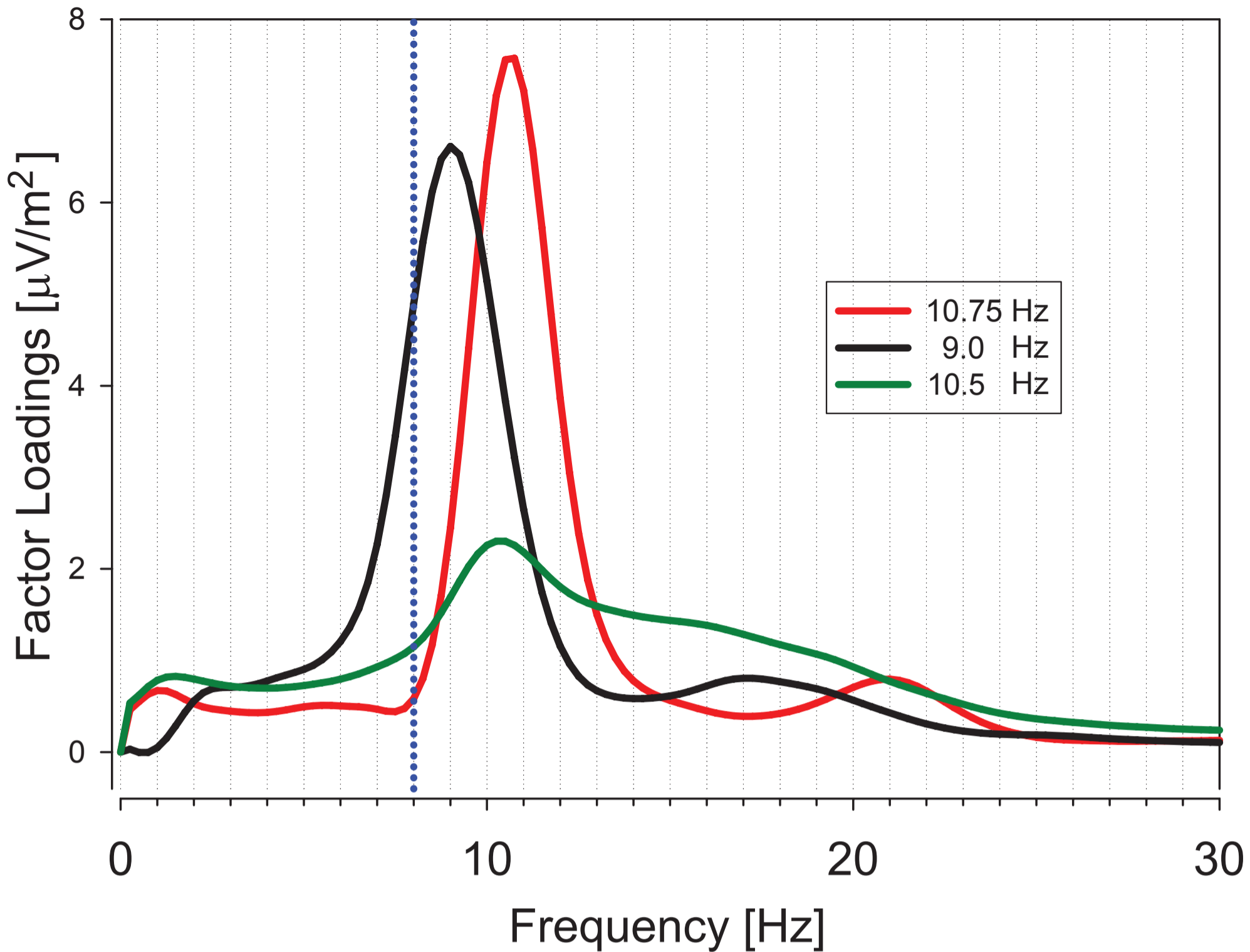


Section S4: fPCA of Low-Density CSD Montage

Although the high-density electrode montage and CSD-fPCA methods provide an advantage for describing and characterizing differences in posterior condition-dependent alpha between responders and nonresponders, a montage consisting of considerably fewer than 67 electrodes should provide acceptable results. We evaluated this possibility by selecting a subset of 16 channels from the full CSD montage, consisting of standard 10-20 sites (F3,Fz,F4; C3,Cz,C4; P7,P3,Pz,P4,P8; O1,Oz,O2), but also including a pair of interpolated sites (PO7/8) to better reflect the posterolateral topography of low-alpha/theta. Data were otherwise processed as indicated in the main analyses. The resulting fPCA factor loadings and eyes-closed topographies are shown in Figure S4.

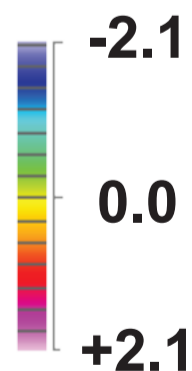
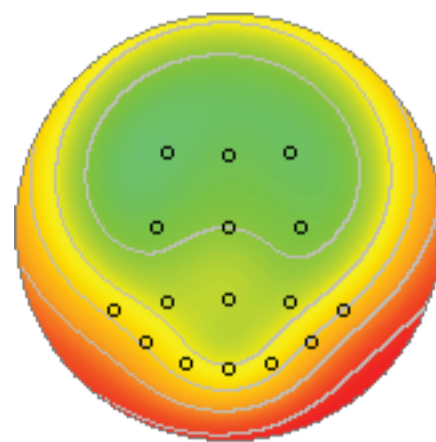
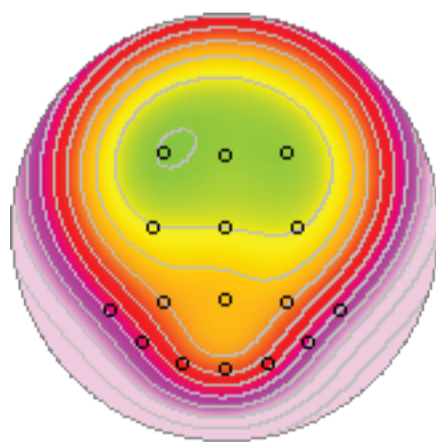
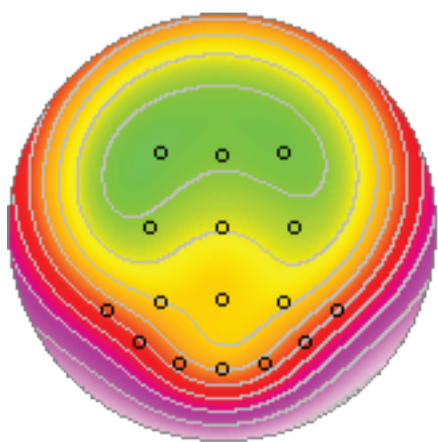
An ANOVA of CSD-fPCA factor score averages across the available posterior sites (P7/8, PO7/8, O1/2, Oz), reproduced the critical *Group x Condition* (3-groups: $F_{[2, 75]} = 4.09$; $p = .021$) and *Response Group x Condition* (2-groups: $F_{[1, 36]} = 7.47$; $p = .01$) seen for the full montage. These data also provided a comparable prediction of treatment response, identifying 15 of the 17 patients with prominent alpha (greater than control median) as responders, but only 13 of 24 with less alpha were responders (Fisher's exact test, 2-tail $p = .022$; positive predictive value = 88.2; specificity = 84.6). The results of the low-density fPCA were therefore comparable with that provided by the complete montage. A necessary caveat is that the spectra for this fPCA were extracted from the complete CSD montage. The adequacy of CSD estimates must also be verified for impoverished montages, which will require additional piloting to validate or optimize the minimal montage required to predict treatment response from posterior, condition-dependent alpha.

Figure S4. The resulting three CSD-fPCA alpha factor loadings are comparable to those derived from the complete montage (cf. Figure 1A) (top panel). Even though the diminished resolution resulted in topographic inaccuracies (cf. Figure S3), the eyes-closed factor score topographies replicated the reduced alpha in nonresponders (bottom panel).

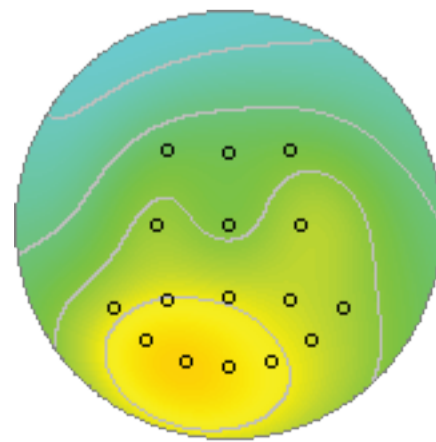
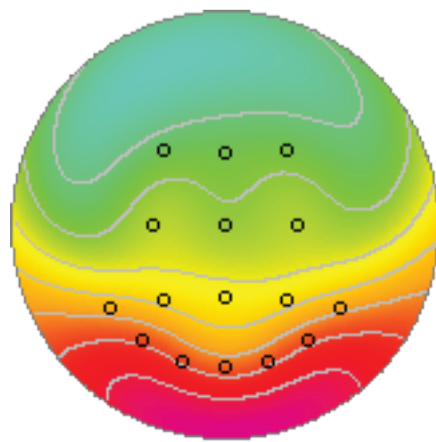
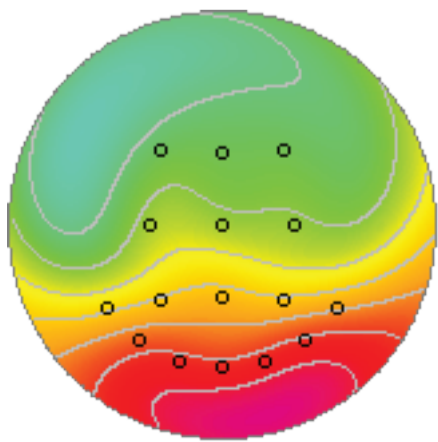


Factor Score Topographies
(Eyes Closed)

Low
Alpha/
Theta
(9.0 Hz)



High
Alpha
(10.75 Hz)



Controls
($n = 41$)

Responders
($n = 28$)

Nonresponders
($n = 13$)

Section S5: Findings for Conventional EEG Analyses

To examine conventional EEG measures, nose-referenced EEG power spectra were computed directly from EEG epochs (1 s, unpadding; 1 Hz FFT resolution), averaged across epochs for each condition, log-transformed, and averaged across subjects in each group (41 controls, 28 responders, 13 nonresponders). The spectral topographies shown in Figure S5 therefore represent conventional log power comparisons common to the literature, and consistent with our prior study (e.g., (2)). Of importance for the present study, controls and responders showed greater eyes-closed alpha than nonresponders throughout the entire 8-12 Hz classic alpha band. However, it should also be noted that this difference is not limited to the alpha band, but starts to build up at 6-8 Hz. Moreover, the anterior midline contribution and posterolateral maximum builds up below 8 Hz, while high-alpha (e.g. 10 Hz) draws toward the posterior midline. These properties are most prominent for eyes-closed, and are characteristic of low-alpha/theta and high-alpha CSD-fPCA factors (cf. Figure 1).

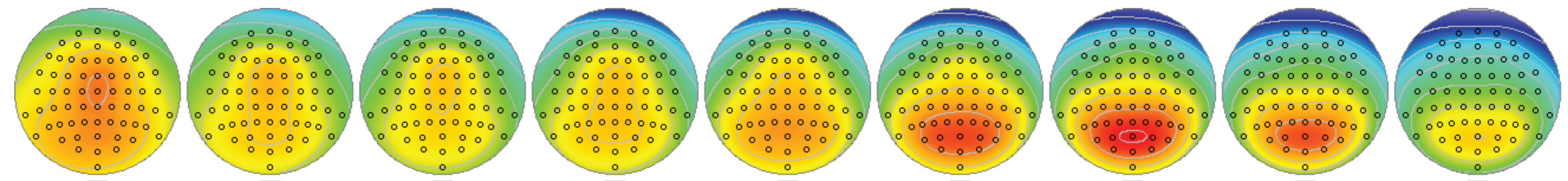
Band-averaged EEG power spectra were also log-transformed and subjected to a conventional repeated measures ANOVA for alpha (8-12 Hz) and theta (4-7 Hz) bands at the medial 10-20 sites (F3/4, C3/4, P3/4, O1/2; cf. (2)), with *Group* (control, nonresponder, responder) as a between-subjects factor and within-subject factors of *Condition* (eyes-open, eyes-closed), *Site* (frontal, central, parietal, occipital), and *Hemisphere* (left, right). In contrast to the CSD-fPCA findings, no statistically significant *Group* (control, responder, nonresponder) effects were observed for alpha; there was no statistical support for an overall difference between groups (the maximal *Group* effect or interaction was *Group*: $F_{[2,79]} = 1.90$, $p = .16$). A statistical trend was also absent when analyses were restricted to patients (i.e., using *Response Group* as a between-subjects factor).

When the same ANOVA model was repeated for the theta band (4-7 Hz spectra in Figure S5), there was no significant *Group* effect, but a *Condition x Site x Group* interaction ($F_{[6, 237]} = 2.93, p = .038, \varepsilon = .484$) was found. As shown in Figure S6, the anterior-to-posterior gradient for condition-dependent theta was more evident in responders and controls than in nonresponders. These topographic and functional properties are similar to those seen for alpha, which strengthens our contention that the EEG differences between SRI responders and nonresponders reflect classic, posterior, condition-dependent (i.e., “visual”) alpha (cf. Figure 1 and Figure S5), which can be measured on either side of the conventional 8 Hz border, and which originates from two distinct spectral components: low-alpha/theta and high-alpha.

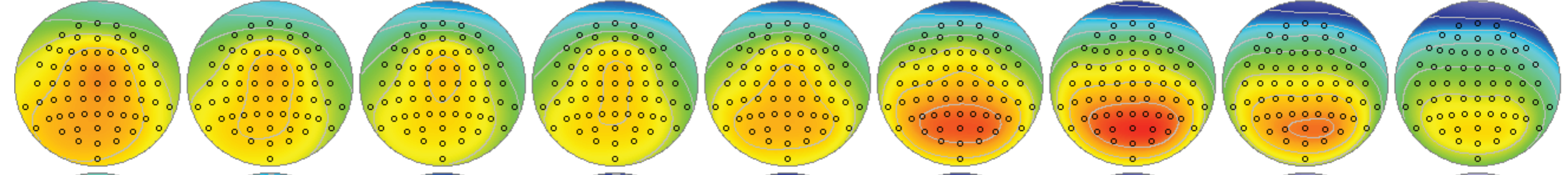
Figure S5. Averaged spectral topographies (nose at top) of eyes-open (top rows) and eyes-closed log EEG power for controls, responders and nonresponders. Columns are unique frequencies ranging from 4-12 Hz.

Eyes Open

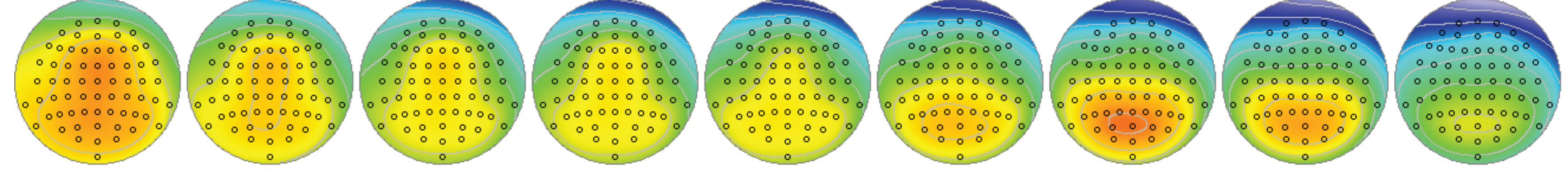
Controls
($n = 41$)



Responders
($n = 28$)



Non-responders
($n = 13$)



4 Hz

5 Hz

6 Hz

7 Hz

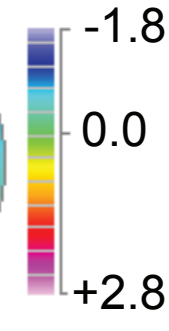
8 Hz

9 Hz

10 Hz

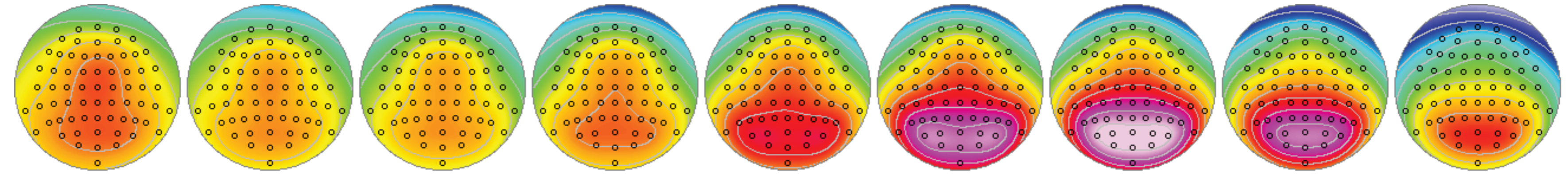
11 Hz

12 Hz

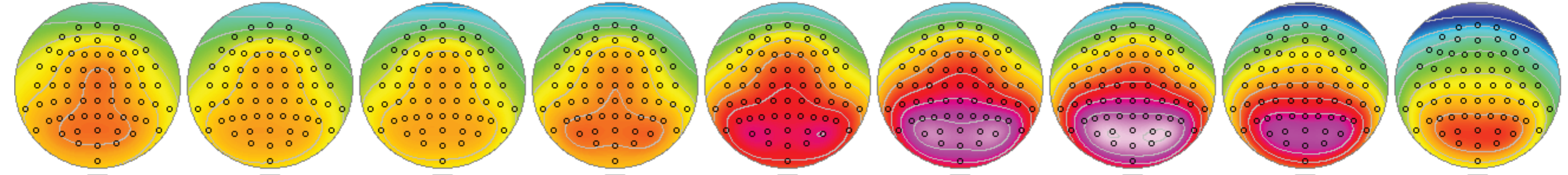


Eyes Closed

Controls
($n = 41$)



Responders
($n = 28$)



Non-responders
($n = 13$)

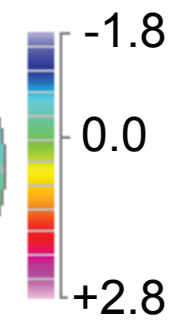
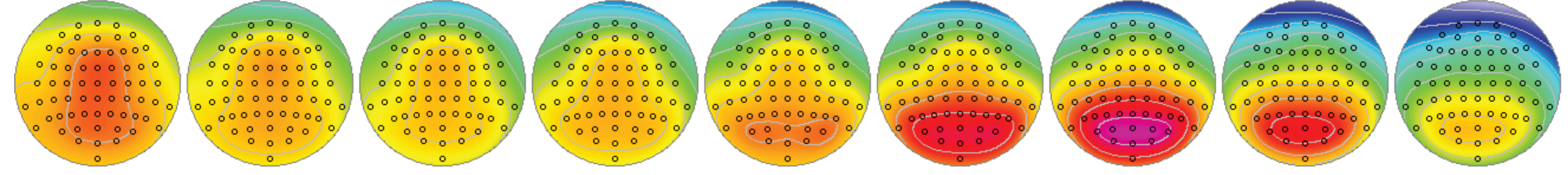
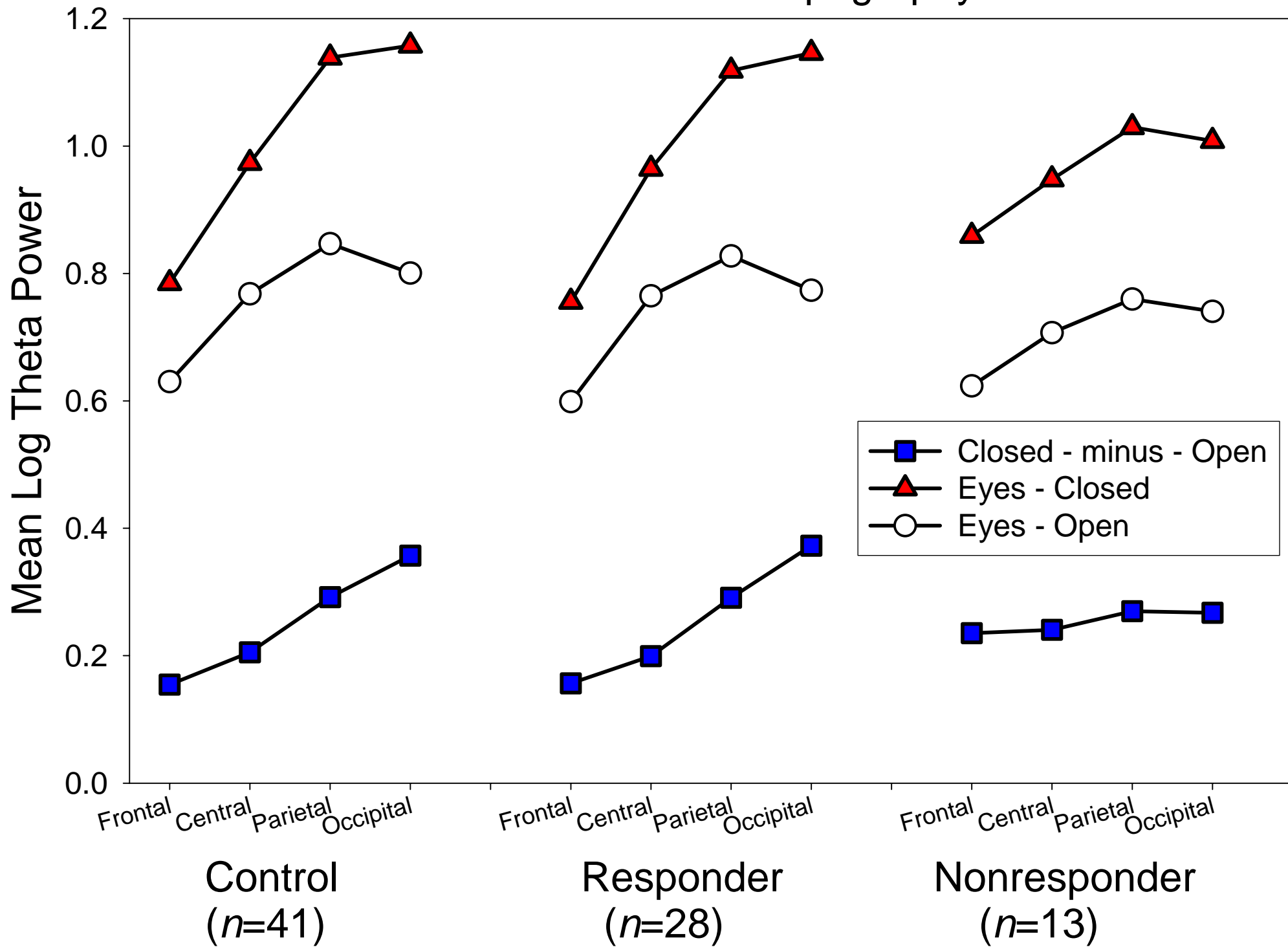


Figure S6. The condition-dependent (eyes-closed minus eyes-open) topography of theta-band activity is consistent with posterior condition-dependent alpha (cf. Figure S5). Both responders and controls showed a monotonic increase in eyes-closed minus eyes-open theta from frontal to occipital sites, which was reduced in nonresponders.

Theta Band EEG Topography



Supplemental References

1. Tenke CE, Kayser J (2005): Reference-free quantification of EEG spectra: combining current source density (CSD) and frequency principal components analysis (fPCA). *Clin Neurophysiol* 116:2826-2846.
2. Bruder GE, Sedoruk JP, Stewart JW, McGrath PJ, Quitkin FM, Tenke CE (2008): Electroencephalographic alpha measures predict therapeutic response to a selective serotonin reuptake inhibitor antidepressant: pre- and post-treatment findings. *Biol Psychiatry* 63:1171-1177.